nature neuroscience

TECHNICAL REPORT

https://doi.org/10.1038/s41593-017-0060-6

# In vivo simultaneous transcriptional activation of multiple genes in the brain using CRISPR–dCas9-activator transgenic mice

Haibo Zhou[1], Junlai Liu[2,3,4], Changyang Zhou[1,3], Ni Gao[1,3], Zhiping Rao[1,3], He Li[1,3], Xinde Hu[1,3], Changlin Li[1], Xuan Yao[1], Xiaowen Shen[1], Yidi Sun[5], Yu Wei[1], Fei Liu[1,3], Wenqin Ying[1], Junming Zhang[1], Cheng Tang[1,3], Xu Zhang[1], Huatai Xu[1], Linyu Shi[1], Leping Cheng[1], Pengyu Huang[2*] and Hui Yang[1*]

**Despite rapid progresses in the genome-editing field, in vivo simultaneous overexpression of multiple genes remains challenging. We generated a transgenic mouse using an improved dCas9 system that enables simultaneous and precise in vivo transcriptional activation of multiple genes and long noncoding RNAs in the nervous system. As proof of concept, we were able to use targeted activation of endogenous neurogenic genes in these transgenic mice to directly and efficiently convert astrocytes into functional neurons in vivo. This system provides a flexible and rapid screening platform for studying complex gene networks and gain-of-function phenotypes in the mammalian brain.**

Neural processing is frequently associated with simultaneous upregulation of numerous genetic elements; thus, overexpression of multiple exogenous genes in vivo is a routine method for probing the causal roles of genetic regulation in the mammalian brain. However, this approach is greatly limited by the size limit of inserted open reading frame (ORF) sequence in the viral expression vectors[1]. Moreover, it is difficult to accurately model the expression of noncoding elements and complex transcript isoform variation using this approach[2,3]. Recently, dCas9-mediated activation has been verified and widely used in different cell lines in vitro[3–21]. An innovative advantage of the dCas9-based activation systems over conventional transgenic techniques is their ability to achieve precise and efficient modulation of multiple loci using a mixture of diverse single-guide RNAs (sgRNAs)[3]. However, in vivo applications of dCas9-activator remain unverified because of ineffective delivery of the large activators and requirement for a more robust transcriptional activation system. Given these limitations, there is an urgent need for a flexible approach to enable efficient dCas9-based activation. We developed a versatile in vivo activation platform and used it to control the transcription of complex genetic elements in the brain.

## Results

**Design of an improved activator platform.** To improve the efficiency of dCas9-fused activators, we established a platform, referred to as SunTag-p65-HSF1 (SPH), by replacing VP64 in SunTag with p65-HSF1, which is used in the synergistic activation mediator (SAM). We hypothesized that GCN4 repeats recruiting multiple copies of p65-HSF1 may induce more potent transcriptional activation (Fig. 1a). To compare the activation potency of SPH with different representative 'second generation' activators[19], we co-transfected human HEK293T and mouse N2a cell lines with *mCherry* driven by a miniCMV promoter, sgRNA targeting the miniCMV promoter and related activators (Supplementary Fig. 1a). Among the examined activator platforms, SPH showed the highest level of activation in both cell lines (Fig. 1b–e and Supplementary Fig. 1b). Notably, mCherry expression was upregulated in 93 ± 1% of the cells expressing the SPH activator system (Supplementary Fig. 2). In addition to exogenous gene, SPH also activated the transcription of the endogenous genes *Ascl1* and *Neurog2* to a higher level in mouse N2a cells as compared with other activators (Fig. 1f and Supplementary Tables 1 and 2). In addition to cell lines, SPH achieved the highest activation in primary astrocytes (Supplementary Fig. 3). An important concern of dCas9 activator system is its specificity in applications. We targeted the exogenous gene *mCherry* and the endogenous gene *Neurog2* to determine SPH's off-target activity using genome-wide transcriptome analysis. We found that SPH specifically activated exogenous and endogenous genes with minimal off-target activity (Fig. 1g,h). Together, these results demonstrate that SPH represents the most potent dCas9 activator system among those examined.

**Generation of a Cre-dependent SPH transgenic mouse and activation of genes and lncRNAs in primary cells and in vivo.** To broadly enable the application of dCas9 in vivo, we generated a Cre-dependent SPH transgenic mouse to overcome the delivery challenges associated with the large sizes of dCas9 and its activators. Using the piggyBac (PB) transposon system, we generated a SPH transgenic mouse containing HA-tagged dCas9 fused with 10xGCN4, which is linked with p65-HSF1 and EGFP in tandem via P2A and T2A, respectively (Fig. 2a). The transgene is driven by the ubiquitous CAG promoter and is interrupted by a *loxP*-stop-*loxP* (LSL) cassette to render Cas9 expression inducible

[1]Institute of Neuroscience, State Key Laboratory of Neuroscience, CAS Center for Excellence in Brain Science and Intelligence Technology, Shanghai Institutes for Biological Sciences, Chinese Academy of Sciences, Shanghai, China. [2]School of Life Science and Technology, ShanghaiTech University, Shanghai, China. [3]College of Life Sciences, University of Chinese Academy of Sciences, Beijing, China. [4]Shanghai Institute of Biochemistry and Cell Biology, Chinese Academy of Sciences, Shanghai, China. [5]Key Lab of Computational Biology, CAS-MPG Partner Institute for Computational Biology, Shanghai Institutes for Biological Sciences, Chinese Academy of Sciences, Shanghai, China. Haibo Zhou, Junlai Liu, Changyang Zhou, Ni Gao, Zhiping Rao and He Li contributed equally to this work. *e-mail: huangpy@shanghaitech.edu.cn; huiyang@ion.ac.cn

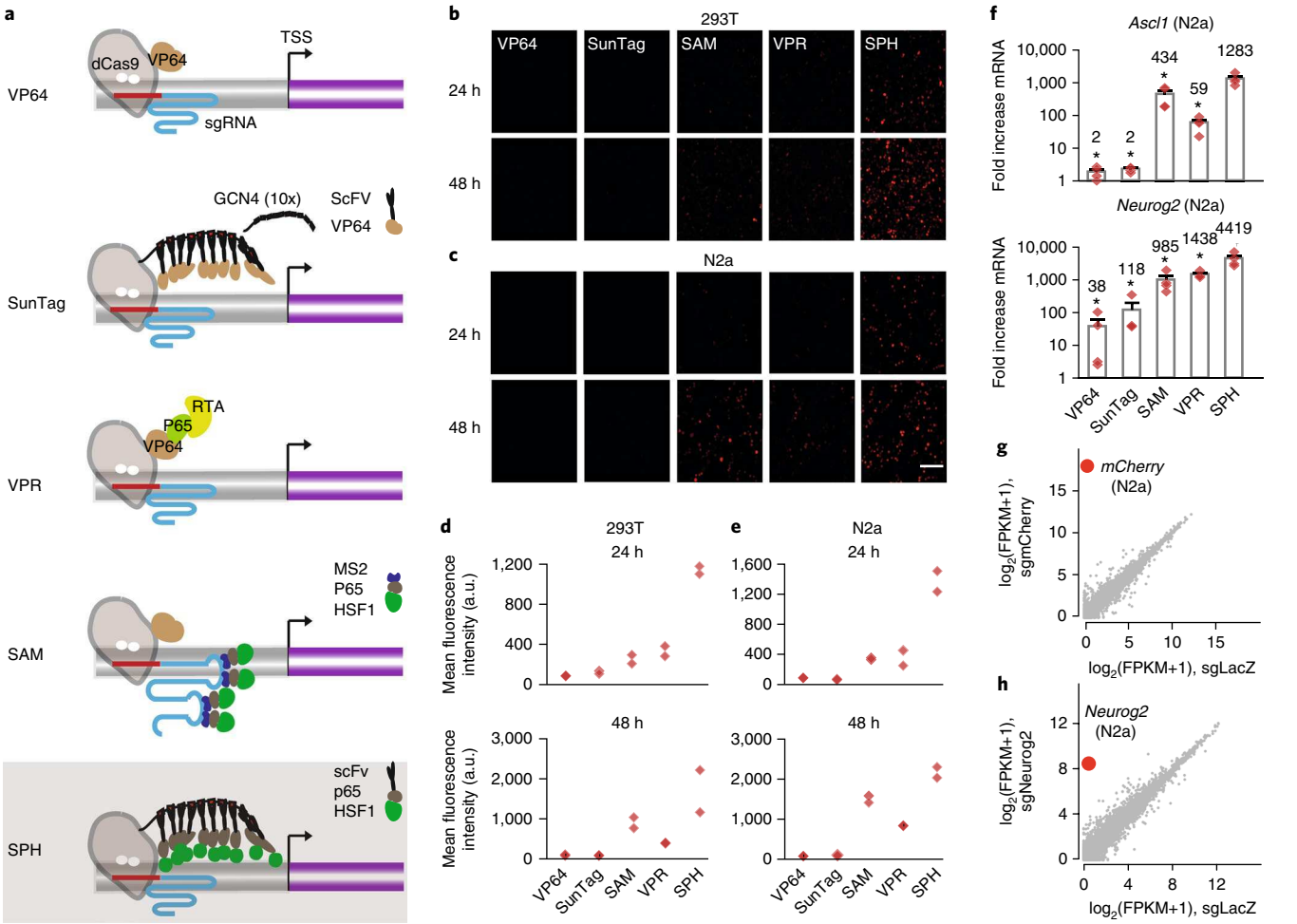


**Fig. 1 | Design of an improved activator SPH. a**, Schematic of five dCas9 activation systems. SPH was designed by combining the peptide array of SunTag and P65-HSF of SAM. **b**,**c**, mCherry driven by a minimal CMV promoter was activated in HEK293T and N2a cells by the indicated dCas9 activation systems. Scale bar represents 100 μm. **d**,**e**, Fluorescent intensity quantifications of the data presented in **b** and **c**. Fold activation of VPR, SunTag, SAM and SPH to VP64 are denoted in the respective graphs ($n=2$ cell cultures). **f**, Activation of endogenous *Ascl1* and *Neurog2* in N2a cells by the indicated dCas9 activation systems; the numbers above the bars indicate the exact fold change (*Ascl1*: $n=4$ cell cultures, $P<0.001$, $f=17.562$, $df=19$; *Neurog2*: $n=4$ cell cultures, $P<0.001$, $f=13.395$, $df=19$; one-way ANOVA followed by Tukey's test). The sgLacZ serves as a control sgRNA. **g**,**h**, Expression levels in $\log_2$FPKM (fragments per kilobase of exon per million fragments mapped) values of all detected genes in RNA-seq libraries of SPH targeting the exogenous gene *mCherry* and the endogenous gene *Neurog2* (*y* axis) compared to LacZ-transfected control (*x* axis). All values are presented as mean ± s.e.m. $^*P<0.05$. TSS, transcription start site.

by Cre recombinase (Fig. 2a). The integration site of SPH was determined and the transgenic progeny were fertile and had normal litter sizes (Supplementary Fig. 4a,b). After transfection with Cre-expression plasmids or infection with Cre-expression virus, dCas9 and EGFP expression could be effectively and specifically induced in vitro and in vivo (Fig. 2c and Supplementary Fig. 4c–g). To determine whether the SPH activator system provided functional expression levels of dCas9 and p65-HSF1, we tested the activation of endogenous genes in primary cells derived from the transgenic mice after infection of U6-sgRNA-Ef1a-Cre-2A-mCherry lentivirus (Fig. 2b). We first targeted two genes encoding neuronal transcription factors, *Ascl1* and *Neurog2*, in primary astrocytes. Both *Ascl1* and *Neurog2* were significantly upregulated (Fig. 2d). We next examined the individual activation of ten genes and four long noncoding RNAs (lncRNAs) and the multiplex activation of ten genes and one lncRNA using a mixture of sgRNAs in primary fibroblasts. All of these genetic elements could be successfully activated at all of the target loci with different sgRNA combinations (Fig. 2e,f). Taken together, our results demonstrate the potential of using SPH mice for efficient gene modulation in primary cells.

To determine the feasibility of using SPH mice to induce transcriptional activation in vivo, we delivered plasmids expressing sgRNAs to the liver by hydrodynamic injection (Supplementary Fig. 5a). Notably, all of the ten genes and one lncRNA (*Miat*) that we analyzed were markedly activated after sgRNA plasmid delivery, with each gene or lncRNA being targeted by one or more sgRNAs (Supplementary Fig. 5b,c). Moreover, via targeted activation of the *Dkk1* gene, which encodes a Wnt antagonist, we remodeled metabolic zonation of the liver and inactivated Wnt/β-catenin downstream pericentral genes, such as glutamine synthetase (GS) and CYP2E1, in about 20% of pericentral hepatocytes (Supplementary Fig. 6), demonstrating that SPH mice can be used to directly modulate cellular processes in vivo.

**In vivo direct conversion of astrocytes into functional neurons by SPH-based targeted activation of endogenous genes.** To demonstrate the potential applications of SPH mice in neuroscience, we

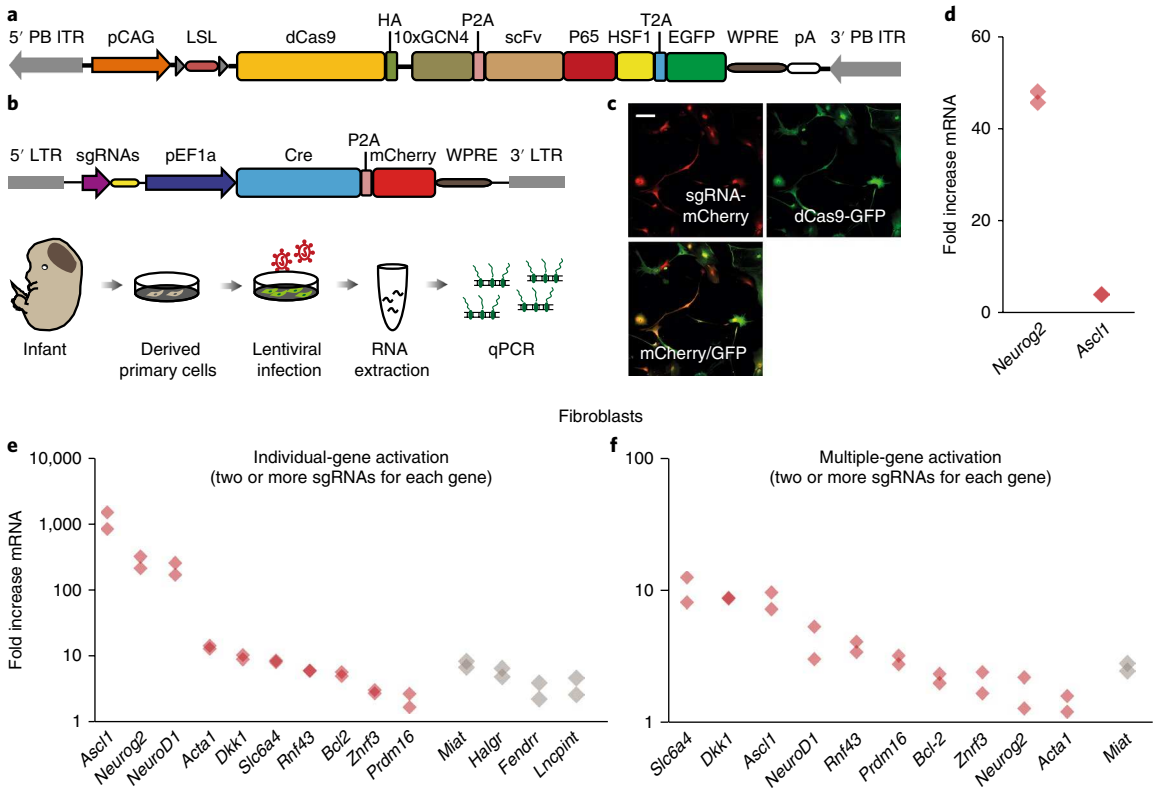


**Fig. 2 | Generation of a Cre-dependent SPH transgenic mouse and activation of genes and lncRNAs in primary cells. a**, Schematic of the Cre-dependent SPH vector used for generating transgenic mice with the piggyBac transposon. **b**, Schematic of the lentiviral vector used for sgRNA expression and experimental flow of gene activations in primary astrocytes derived from SPH transgenic mice. **c**, Immunofluorescence images of primary SPH astrocytes infected with lentivirus expressing Cre recombinase ($n=1$ cell culture). Scale bar represents 50 μm. **d**, Induction of two genes encoding neural transcription factors, *Ascl1* and *Neurog2*, in primary astrocytes ($n=2$ cell cultures). **e**, Activation of ten genes and four lncRNAs individually ($n=2$ cell cultures). **f**, Multiplex activation of ten genes and one lncRNA simultaneous with a mixture of sgRNA-expressing lentivirus ($n=2$ cell cultures). The sgLacZ serves as a control sgRNA.

asked whether the SPH transgenic mice can be used to modulate neuronal functions in vivo. Ectopic overexpression of transgenes is often applied to reprogram cell fates. A previous study used dCas9 to reprogram fibroblasts into neurons (iNs) in vitro[20]. We explored the possibility of in vivo direct conversion of mature astrocytes into iNs by SPH-based targeted activation of three previously described[22–24] neurogenic transcription factors: *Ascl1*, *Neurog2* and *Neurod1* (ANN) (Fig. 3a and Supplementary Table 3). The ANN factors were efficiently activated in primary SPH astrocytes after transfection of plasmids expressing Cre and sgRNAs (Fig. 3b). In addition, we generated SPH;GFAP-Cre double-transgenic mice to induce SPH activator systems in astrocytes. To induce neuronal conversion of astrocytes in vivo, we delivered AAV-sgRNAs targeting ANN factors, with each gene being targeted by multiple sgRNAs. AAV-GFAP-mCherry was also co-injected with AAV-sgRNAs to label astrocytes in the midbrain[22]. All of the ANN factors were efficiently activated in the midbrain by 1 week after AAV injection (Fig. 3c). A significantly increased proportion of mCherry$^+$ NeuN$^+$ cells was induced 1 month after AAV injection compared with control left midbrain injected with only AAV-GFAP–mCherry: 34 ± 8% versus 5 ± 1% (Fig. 3d–f). To characterize the functions of iNs induced by targeted ANN activation, we performed whole-cell recordings in acute slices to examine the electrophysiological properties of iNs generated in vivo. Morphology and mCherry expression were used to select mature iNs for patch-clamp recordings (Fig. 3g). All of the recorded cells ($n=5$ cells) were able to generate action potentials in response to step injection of depolarizing current in current-clamp mode (Fig. 3h). Moreover, all of the cells displayed spontaneous postsynaptic currents in voltage-clamp mode (Fig. 3i), suggesting that iNs form functional synapses.

**Complex activation in the mammalian brain.** Simultaneous expression of multiple genes is frequently required to modulate neuronal processes. However, in vivo modulation of multiple targets is largely limited by inefficient delivery of multiple constructs, especially genes with large transcript size. CRISPR–dCas9 activators have been developed for multiple transcriptional activations[3]. Using SPH mice, we achieved robust activation of multiple genes in the liver with a mixture of sgRNAs (Supplementary Fig. 5d). To avoid mosaic activations, we also introduced a sgRNA array to enable simultaneous activation of multiple genes and lncRNAs in a cell. After prescreen of sgRNAs in N2a cells and primary SPH fibroblasts (Supplementary Fig. 7), ten sgRNAs targeting the promoters of eight genes and two lncRNAs were selected and constructed into an sgRNA array, with each genetic element being targeted by one sgRNA (Supplementary Fig. 8a and Supplementary Table 4). Notably, all of the targets were simultaneously activated after injection of the plasmids into the liver (Supplementary Fig. 8b). Moreover, AAVs expressing sgRNA arrays enabled simultaneous activation of multiple targets in SPH livers together with AAV-Alb-Cre (Supplementary Fig. 9). To further confirm the simultaneous activation of multiple targets at single-cell level, we prepared primary astrocytes transfected with all-in-one vectors for single-cell RNA sequencing. As a result of detection limits, we detected three of the eight targeted genes. All of the detected genes were simultaneously upregulated in almost all of the cells (Supplementary Fig. 10).

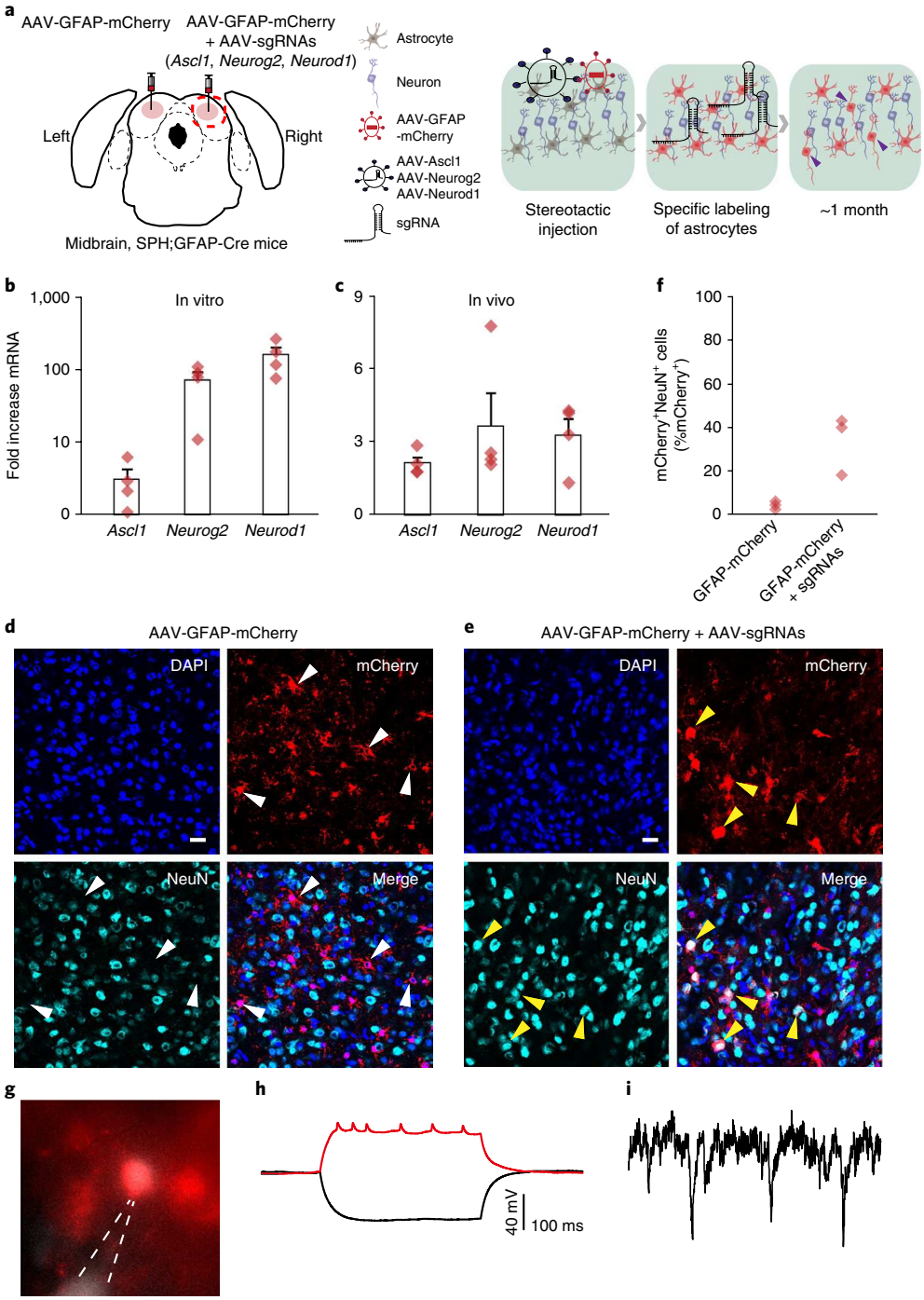


**Fig. 3 | SPH-based targeted activations convert astrocytes into functional neurons in vivo. a**, Schematic of injection strategies. Dorsal midbrain was injected with AAV-GFAP-mCherry and AAV-sgRNAs targeting ANN factors on the right side and AAV-GFAP-mCherry as a control on the left side. **b**, Transcriptional activation of ANN factors in primary SPH astrocytes ($n = 4$ cell cultures, 2–3 d post-transfection). **c**, Transcriptional activation of ANN factors in the dorsal midbrain ($n = 4$ mice, 1 week after infection). **d**,**e**, Representative immunofluorescence images of the midbrain 1 month post-infection ($n = 3$ mice, AAV-GFAP-mCherry: 5 images; AAV-GFAP-mCherry + AAV-sgRNAs: 5 images). White arrowheads indicate that mCherry and NeuN expression was not colocalized. Note that NeuN is a marker of mature neurons. Orange arrowheads indicate colocalization of mCherry and NeuN. **f**, Percentage of mCherry$^+$ NeuN$^+$ double-positive cells in mCherry$^+$ cells 1 month post-infection ($n = 3$ mice; $P = 0.02$, $t = -3.71$, $df = 5$, unpaired two-tailed Student's $t$ test). **g**, Whole-cell recording of a representative iN in the acute slice ($n = 2$ mice, 5 cells). **h**,**i**, Action potentials were evoked in response to step depolarizing currents and synaptic inputs were detected from the same iN ($n = 2$ mice, 5 cells). All values are presented as mean ± s.e.m. $^*P < 0.05$. Scale bars represent 20 μm in **d**, **e** and **g**.

The brain is composed of numerous types of neuronal cells. Precise interrogation of the genetic circuits is important to understand how the brain processes. With the conditional SPH mouse, cell-type-specific activation of multiple genes can be defined by delivering Cre recombinase under the control of specific promoters. To determine whether cell-type-specific activation of multiple genomic loci can be achieved in the intact brain, we constructed a dual-vector system that packages sgRNAs and Cre recombinase

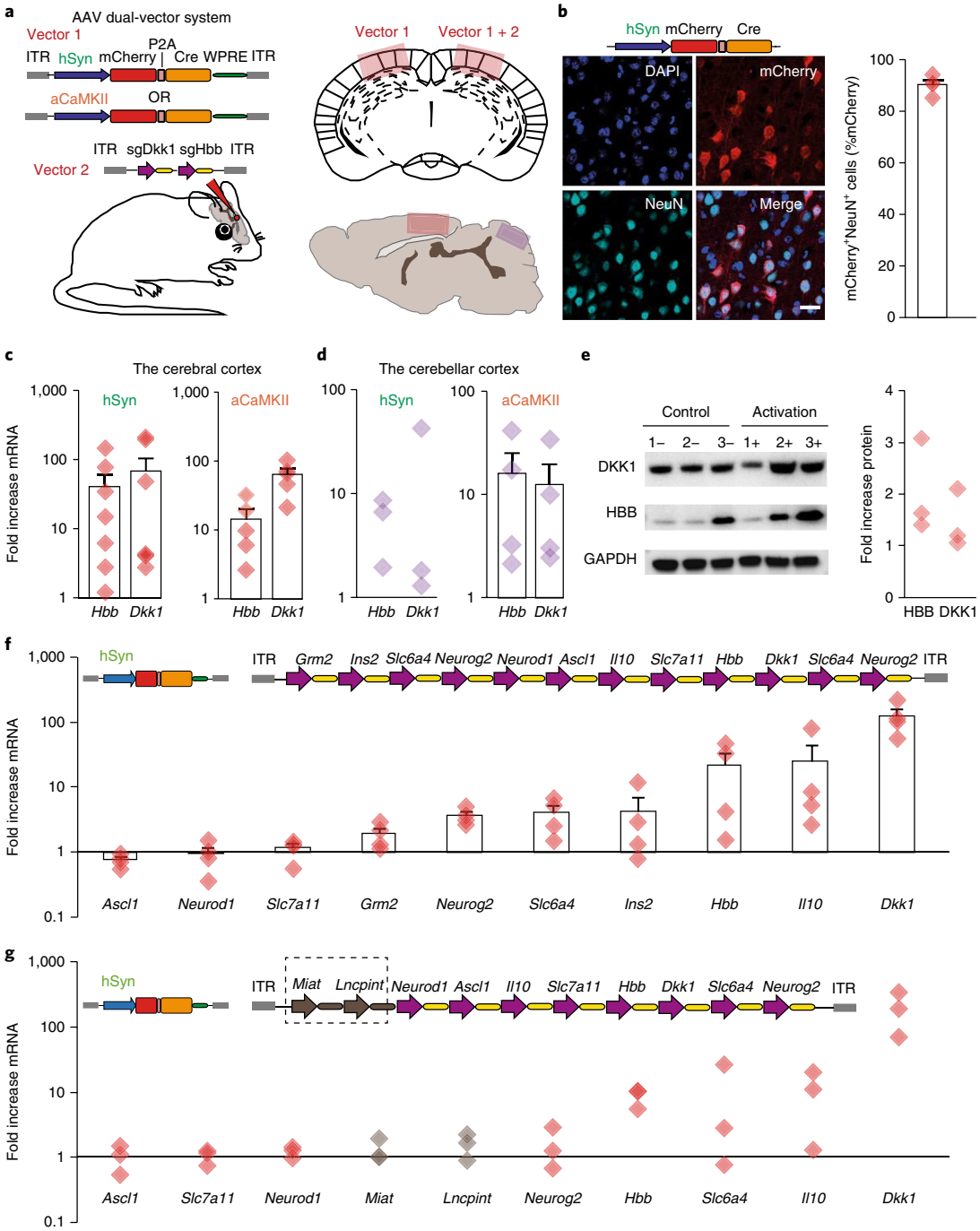


**Fig. 4 | Complex transcriptional activation in the intact brain using a single sgRNA array. a**, Schematic illustration showing stereotactic injection of dual-AAV vectors expressing Cre and sgRNAs into the cerebral cortex (red) or cerebellar cortex (purple) of Cre-dependent SPH mice. Note that vector 1 serves as a control and aCaMKII is an excitatory-neuron-specific promoter. **b**, Immunostaining of the cerebral cortex 1–2 weeks post-transduction revealed that AAV-hSyn-Cre expression was highly colocalized with NeuN expression ($n=4$ mice). Scale bar represents 20 μm. **c**, Neuron-specific and excitatory-neuron-specific activation of *Dkk1* and *Hbb* in the cerebral cortex driven by a human synapsin promoter (hSyn) ($n=7$ mice) and aCaMKII promoters ($n=5$ mice), respectively. **d**, Neuron-specific and excitatory-neuron-specific activation of *Dkk1* and *Hbb* in the cerebellar cortex driven by hSyn ($n=3$ mice) and aCaMKII promoters ($n=4$ mice), respectively. **e**, Simultaneous upregulation of HBB and DKK1 proteins after injecting AAV-aCaMKII-Cre in the cerebral cortex ($n=3$ mice). Gel images were cropped. **f**, Schematic of the sgRNA array targeting ten genes and activation of all targets in the brain simultaneously ($n=4$ mice). *Slc6a4* and *Neurog2* sgRNAs in the sgRNA array were replicated to two copies as a result of homologous recombination during plasmid preparation. **g**, Schematic of the sgRNA array targeting eight genes and two lncRNAs and activation of all targets in the brain simultaneously ($n=3$ mice). lncRNAs are highlighted by the dashed line boxes. All values are presented as mean ± s.e.m.

driven by a specific promoter in two separate AAV vectors. We injected dual-AAV vectors in the cerebral and cerebellar cortex: one expressing sgRNAs targeting *Dkk1* and *Hbb*, and another expressing Cre recombinase linked with *mCherry* in tandem via P2A, specifically expressed in neurons (hSyn-Cre) or excitatory neurons (aCaMKII-Cre) (Fig. 4a). We dissected the injected brain regions

for qPCR analysis 1–2 weeks after injection of AAV-hSyn-Cre and AAV-sgDkk1-sgHbb. Activation of *Dkk1* and *Hbb* was detected in both cerebral cortex and cerebellar cortex and most mCherry-positive cells were colocalized with NeuN expression, suggesting that activation of the sites targeted by sgRNAs was restricted to neurons (Fig. 4b–d). Upregulations of *Dkk1* and *Hbb* were also detected in the cerebral cortex and cerebellar cortex by injection of AAV-aCaMKII-Cre and AAV-sgDkk1-sgHbb (Fig. 4c,d). Enhanced transcription of *Dkk1* and *Hbb* were confirmed by in situ hybridization (Supplementary Fig. 11 and Supplementary Table 5). Moreover, we observed simultaneous upregulation of HBB and DKK1 proteins after injecting AAV-aCaMKII-Cre together with related sgRNAs in the cerebral cortex, confirming SPH-based targeted activation of genes in protein levels (Fig. 4e and Supplementary Fig. 12).

Many neuronal processes are regulated by the gene network. Thus, simultaneous adjustment of a large number of genes could be used to determine the causal roles of complex genetic regulation. To characterize the feasibility of using SPH mice to simultaneously control multiple genes in vivo, we injected sgRNA arrays targeting ten genes or ten genetic elements including eight genes and two lncRNAs into the brain (Fig. 4f,g). As expected, most of the targets were potently upregulated (Fig. 4f,g). Collectively, these results highlight the advantages and potential of using SPH mice to modulate complex genetic networks in the intact brain.

## Discussion

We developed an efficient and versatile platform for simultaneous activation of multiple genomic loci in the intact nervous system. Using this SPH platform, we potently upregulated individual or multiple genetic elements both ex vivo and in vivo using a mixture of sgRNAs. The traditional method of gene overexpression by ectopic expression of exogenous transgenes usually introduces multiple copies of genes[20,25,26]. In contrast, activation of endogenous genes by dCas9 activators potentially reflects a more natural mechanism of action. Notably, SPH activator system enables in vivo dissections of diverse types of genetic elements, such as lncRNAs and transcription variants that are often not suitable for ectopic expression. Moreover, targeted activation of ANN factors converts astrocytes into functional neurons in the midbrain, suggesting that endogenous genes activated by SPH-based strategy function in vivo. To the best of our knowledge, this is the first use of dCas9-based technologies to induce a functional phenotype in higher animals.

Many neurological diseases are correlated with aberrant expressions of multiple genes. Targeting a single gene is usually insufficient to model the pathological processes. Thus, SPH-mouse-based in vivo multiplex activation potentially provides a platform for better disease modeling. The SPH mouse is also particularly useful for in vivo cell reprogramming. A cocktail of transcriptional factors is often used to initiate cell fate conversion[27]. Although cell fate conversions in cell culture have been reported in many studies, in vivo transdifferentiation remains challenging as a result of difficulties in simultaneous expression of several exogenous genes in intact tissues[27]. Thus, the SPH-mouse-based strategy enables in vivo reprogramming. We generated iNs in SPH mouse midbrains by targeted activation of three transcription factors using a mixture of sgRNAs. Future work will be needed to determine whether specific subtypes of neural cells can be converted using a sgRNA array. Given that all biological activity is virtually modulated by the interactions of multiple genes, SPH-mouse-mediated simultaneous activation is potentially applicable to many fields beyond disease modeling and cell reprogramming.

We also noticed that genes were activated at different levels in SPH platform, which has also been shown in other dCas9-based activation systems[3,19]. The different extents of gene activation are probably a result of their basal expression levels, epigenetic status or sgRNA target sites[3,19,28,29]. SPH-mediated multiplex activation allows fine-tuning of individual gene expression by targeting upstream of the transcription start site with different sgRNAs or different combinations of sgRNAs[30]. Thus, the SPH platform provides an alternative strategy for studying the effect of mRNA dosage of individual gene in complex biological processes. For genes with limited activation efficiency, modest activations of some genes, such as *Mecp2* and *Shank3*, could also be sufficient to induce physiological changes of neurons[31–33]. It is also important to note that we examined the efficacy of SPH system in neurons and astrocytes, which are the representative cell types in the brain. The efficacy of SPH system in other types of glial cells, such as oligodendrocytes and microglia, should be examined before applying the SPH system to other neural cell types in vivo.

In addition to investigating a small set of genes, a special application of SPH mice would be in vivo genome-wide gain-of-function screens. Recently, in vitro dCas9-based activation screens have been used to identify key regulators involved in a variety of biological processes[3,27,34–36]. Given the recent success of using Cas9-expressing mice to screen tumor suppressor genes in glioblastoma[37], SPH mice could be used to identify oncogenes involved in the progression of diverse tumors. Together, SPH mouse provides a gain-of-function platform for dissecting complex genetic processes under physiological conditions.

## Methods

Methods, including statements of data availability and any associated accession codes and references, are available at https://doi.org/10.1038/s41593-017-0060-6.

Received: 5 April 2017; Accepted: 7 December 2017;
Published online: 15 January 2018

## References

1. Wu, Z., Yang, H. & Colosi, P. Effect of genome size on AAV vector packaging. *Mol. Ther.* **18**, 80–86, https://doi.org/10.1038/mt.2009.255 (2010).
2. Shechner, D. M., Hacisuleyman, E., Younger, S. T. & Rinn, J. L. Multiplexable, locus-specific targeting of long RNAs with CRISPR-Display. *Nat. Methods* **12**, 664–670, https://doi.org/10.1038/Nmeth.3433 (2015).
3. Konermann, S. et al. Genome-scale transcriptional activation by an engineered CRISPR-Cas9 complex. *Nature* **517**, 583–588, https://doi.org/10.1038/nature14136 (2015).
4. Zetsche, B., Volz, S. E. & Zhang, F. A split-Cas9 architecture for inducible genome editing and transcription modulation. *Nat. Biotechnol.* **33**, 139–142 (2015).
5. Dahlman, J. E. et al. Orthogonal gene knockout and activation with a catalytically active Cas9 nuclease. *Nat. Biotechnol.* **34**, 441–441 (2016).
6. Qi, L. S. et al. Repurposing CRISPR as an RNA-guided platform for sequence-specific control of gene expression. *Cell* **152**, 1173–1183, https://doi.org/10.1016/j.cell.2013.02.022 (2013).
7. Gilbert, L. A. et al. CRISPR-mediated modular RNA-guided regulation of transcription in eukaryotes. *Cell* **154**, 442–451, https://doi.org/10.1016/j.cell.2013.06.044 (2013).
8. Tanenbaum, M. E., Gilbert, L. A., Qi, L. S., Weissman, J. S. & Vale, R. D. A protein-tagging system for signal amplification in gene expression and fluorescence imaging. *Cell* **159**, 635–646, https://doi.org/10.1016/j.cell.2014.09.039 (2014).
9. Perez-Pinera, P. et al. RNA-guided gene activation by CRISPR-Cas9-based transcription factors. *Nat. Methods* **10**, 973–976, https://doi.org/10.1038/Nmeth.2600 (2013).
10. Gilbert, L. A. et al. Genome-scale CRISPR-mediated control of gene repression and activation. *Cell* **159**, 647–661, https://doi.org/10.1016/j.cell.2014.09.029 (2014).
11. Zalatan, J. G. et al. Engineering complex synthetic transcriptional programs with CRISPR RNA scaffolds. *Cell* **160**, 339–350, https://doi.org/10.1016/j.cell.2014.11.052 (2015).
12. Polstein, L. R. & Gersbach, C. A. A light-inducible CRISPR-Cas9 system for control of endogenous gene activation. *Nat. Chem. Biol.* **11**, 198–200, https://doi.org/10.1038/nchembio.1753 (2015).
13. Cheng, A. W. et al. Multiplexed activation of endogenous genes by CRISPR-on, an RNA-guided transcriptional activator system. *Cell. Res.* **23**, 1163–1171, https://doi.org/10.1038/cr.2013.122 (2013).

14. Gao, Y. et al. Complex transcriptional modulation with orthogonal and inducible dCas9 regulators. *Nat. Methods* **13**, 1043–1049, https://doi.org/10.1038/nmeth.4042 (2016).
15. Maeder, M. L. et al. CRISPR RNA-guided activation of endogenous human genes. *Nat. Methods* **10**, 977–979, https://doi.org/10.1038/Nmeth.2598 (2013).
16. Bikard, D. et al. Programmable repression and activation of bacterial gene expression using an engineered CRISPR-Cas system. *Nucleic Acids Res.* **41**, 7429–7437, https://doi.org/10.1093/nar/gkt520 (2013).
17. Mali, P. et al. CAS9 transcriptional activators for target specificity screening and paired nickases for cooperative genome engineering. *Nat. Biotechnol.* **31**, 833–838, https://doi.org/10.1038/nbt.2675 (2013).
18. Chavez, A. et al. Highly efficient Cas9-mediated transcriptional programming. *Nat. Methods* **12**, 326–328, https://doi.org/10.1038/Nmeth.3312 (2015).
19. Chavez, A. et al. Comparison of Cas9 activators in multiple species. *Nat. Methods* **13**, 563–567, https://doi.org/10.1038/Nmeth.3871 (2016).
20. Black, J. B. et al. Targeted epigenetic remodeling of endogenous loci by CRISPR/Cas9-based transcriptional activators directly converts fibroblasts to neuronal cells. *Cell. Stem Cell.* **19**, 406–414, https://doi.org/10.1016/j.stem.2016.07.001 (2016).
21. Nihongaki, Y. et al. CRISPR-Cas9-based photoactivatable transcription systems to induce neuronal differentiation. *Nat. Methods* **14**, 963–966, https://doi.org/10.1038/nmeth.4430 (2017).
22. Liu, Y. et al. Ascl1 converts dorsal midbrain astrocytes into functional neurons in vivo. *J. Neurosci.* **35**, 9336–9355, doi:https://doi.org/10.1523/Jneurosci.3975-14.2015 (2015).
23. Heinrich, C. et al. Directing astroglia from the cerebral cortex into subtype specific functional neurons. *PLoS. Biol.* **8**, e1000373, https://doi.org/10.1371/journal.pbio.1000373 (2010).
24. Cheng, L. et al. Direct conversion of astrocytes into neuronal cells by drug cocktail. *Cell. Res.* **25**, 1269–1272, https://doi.org/10.1038/cr.2015.120 (2015).
25. Davis, R. L., Weintraub, H. & Lassar, A. B. Expression of a single transfected cDNA converts fibroblasts to myoblasts. *Cell* **51**, 987–1000, doi:https://doi.org/10.1016/0092-8674(87)90585-X (1987).
26. Takahashi, K. & Yamanaka, S. Induction of pluripotent stem cells from mouse embryonic and adult fibroblast cultures by defined factors. *Cell* **126**, 663–676, https://doi.org/10.1016/j.cell.2006.07.024 (2006).
27. Mertens, J., Marchetto, M. C., Bardy, C. & Gage, F. H. Evaluating cell reprogramming, differentiation and conversion technologies in neuroscience. *Nat. Rev. Neurosci.* **17**, 424–437, https://doi.org/10.1038/nrn.2016.46 (2016).
28. Hilton, I. B. et al. Epigenome editing by a CRISPR-Cas9-based acetyltransferase activates genes from promoters and enhancers. *Nat. Biotechnol.* **33**, 510–517, https://doi.org/10.1038/nbt.3199 (2015).
29. Liu, X. S. et al. Editing DNA methylation in the mammalian genome. *Cell* **167**, 233–247.e17, https://doi.org/10.1016/j.cell.2016.08.056 (2016).
30. Farzadfard, F., Perli, S. D. & Lu, T. K. Tunable and multifunctional eukaryotic transcription factors based on CRISPR/Cas. *ACS Synth. Biol.* **2**, 604–613, https://doi.org/10.1021/sb400081r (2013).
31. Han, K. et al. SHANK3 overexpression causes manic-like behavior with unique pharmacogenetic properties. *Nature* **503**, 72–77, https://doi.org/10.1038/nature12630 (2013).
32. Lombardi, L. M., Baker, S. A. & Zoghbi, H. Y. MECP2 disorders: from the clinic to mice and back. *J. Clin. Invest.* **125**, 2914–2923, https://doi.org/10.1172/JCI78167 (2015).
33. Collins, A. L. et al. Mild overexpression of MeCP2 causes a progressive neurological disorder in mice. *Hum. Mol. Genet.* **13**, 2679–2689, https://doi.org/10.1093/hmg/ddh282 (2004).
34. Joung, J. et al. Genome-scale activation screen identifies a lncRNA locus regulating a gene neighborhood. *Nature* **548**, 343–346, https://doi.org/10.1038/nature23451 (2017).
35. Horlbeck, M. A. et al. Compact and highly active next-generation libraries for CRISPR-mediated gene repression and activation. *Elife* **5**, e19760, https://doi.org/10.7554/eLife.19760 (2016).
36. Simeonov, D. R. et al. Discovery of stimulation-responsive immune enhancers with CRISPR activation. *Nature* **549**, 111–115, https://doi.org/10.1038/nature23875 (2017).
37. Chow, R. D. et al. AAV-mediated direct in vivo CRISPR screen identifies functional suppressors in glioblastoma. *Nat. Neurosci.* **20**, 1329–1341, https://doi.org/10.1038/nn.4620 (2017).


## Acknowledgements

We thank D. Li, E. Zuo, Y. Shi, Y. Liu, J. He, J. Pan, Y. Zhong, Y. Lu, Y. Zhang, J. Yang and X. Tang for technical assistance and valuable discussion. This work was supported by National Science and Technology Major Project (2017YFC1001302), CAS Strategic Priority Research Program (XDB02050007, XDA01010409), the MoST863 Program (2015AA020307), NSFC grants (31522037, 31500825, 31571509, 31522038), China Youth Thousand Talents Program (to H.Y.), Break through project of Chinese Academy of Sciences, Shanghai Sailing Plan for the Young Scientific Talents (15YF1414700), and The Ministry of Science and Technology of China (MOST; 2016YFA0100500).

## Author contributions

H.Z. designed and performed the experiments. J.L. designed and performed the in vivo gene activation in the liver and western blot. C.Z. designed the SPH activation system. N.G., H.L., X.H. and J.Z. cloned the vectors, and performed and analyzed the gene activation experiments in vitro, ex vivo and in vivo. X.S. and L.S. produced AAV8. Z.R., L.C. and F.L. designed and performed the in situ hybridization, ex vivo activation of Ascl1 and Neurog2 in astrocytes and assisted with the in vivo conversion experiments. C.L. and X.Z. performed single-cell RNA sequencing, Y.S. analyzed RNA sequencing and single-cell RNA-sequencing data. H.X. performed electrophysiology. Y.W., X.Y. and W.Y. generated the SPH transgenic mice. C.T. assisted with the immunofluorescence staining of brains and livers. P.H. designed and supervised the experiments of in vivo activation in SPH mice. H.Y. supervised the project and designed experiments. H.Z., P.H. and H.Y. wrote the manuscript.

## Competing interests

The authors declare no competing financial interests.

## Additional information

**Supplementary information** is available for this paper at https://doi.org/10.1038/s41593-017-0060-6.

**Reprints and permissions information** is available at www.nature.com/reprints.

**Correspondence and requests for materials** should be addressed to P.H. or H.Y.

**Publisher's note:** Springer Nature remains neutral with regard to jurisdictional claims in published maps and institutional affiliations.

## Methods

**Ethical compliance.** All animal experiments were performed and approved by the Animal Care and Use Committee of the Institute of Neuroscience, Chinese Academy of Sciences, Shanghai, China.

**sgRNA design and vector information.** The sgRNAs were designed using the ChopChop tool (https://chopchop.rc.fas.harvard.edu/). All sgRNAs used in this project are listed in Supplementary Table 1. DNA sequences of all vectors are provided in the Supplementary Sequences.

**Cell culture and transient transfection.** HEK293T and N2a cell lines were cultured in Dulbecco's Modified Eagle Medium (DMEM) supplemented with 10% FBS and penicillin/streptomycin (Thermo Fisher Scientific) in a humidified incubator at 37 °C with 5% $CO_2$. Cells were passaged at a ratio 1:3 every 2 d. HEK293T and N2A Cell lines were seeded in 24-well plates or 12-well plates, with the purpose of performing fluorescence reporter assay or activation of endogenous genes, respectively. All cell lines were transfected with Lipofectamine 3000 (Thermo Fisher Scientific) using the standard protocol.

**Fluorescence reporter assay and activation of endogenous gene in vitro.** The experiments were performed using previously described methods with modifications[18,19]. For the experiments of fluorescence reporter assay, each well was transfected with 1 μg of plasmid with dCas9, 1 μg of activator expressing plasmid, 0.5 μg of plasmid containing sgRNA and 0.5 μg of miniCMV plasmid. Considering VP64 system does not require an extra vector to express activator, the activator expressing plasmid was substituted by same amount of an empty vector pcDNA3.1(+). In addition, 0.5 μg of plasmid expressing blue fluorescence protein (BFP) was co-transfected per well to control the transfection efficiency. The mean fluorescence intensity of mCherry was determined by measuring the mCherry intensity of randomly selected BFP-positive cells. Images were acquired using A1R microscope (Nikon) with identical settings at 24 h or 48 h, respectively.

For endogenous gene activation experiments, each well was transfected with 1 μg of plasmid with dCas9, 0.09 pM of plasmid containing sgRNA and 1 μg of activator expressing plasmid (substituted by 1 μg of pcDNA3.1(+) in the VP64 system and VPR system). Cells were harvested 2–3 d post-transfection.

To determine the activation of *Ascl1*, *Neurog2* and *Neurod1* in primary astrocytes, each well (six-well plate) was transfected with 1 μg of plasmid expressing EF1a-Cre-mCherry and 3 μg of plasmid containing sgRNAs. mCherry –positive cells were collected by fluorescence-activated cell sorting (FACS) 2 d post-transfection.

**Generation of the SPH transgenic mouse.** The sequence of SPH is available in Supplementary Sequences. Cre-dependent SPH transgenic mice were generated with the piggyBac transposon system in $F_1$ zygotes, as described previously[38]. Three chimeric male founders were selected to cross with wild type C57BL/6 mice. Primers used for determining the SPH-positive mice were forward (5′-TTCCATTTCAGGTGTCGTGA-3′) and reverse (5′-ACCAGCTGGATGAACAGCTT-3′). SPH;Alb-Cre double-transgenic mice were generated by crossing SPH transgenic mice with Alb-Cre (C57BL/6 background, forward primer: 5′-GCCTGCATTACCGGTCGATGC-3′ and reverse primer: 5′- CAGGGTGTTATAAGCAATCCCC -3′) transgenic mice. And SPH;GFAP-Cre double-transgenic mice were generated by crossing SPH transgenic mice with GFAP-Cre (JAX stock #004600,forward primer: 5′-GCCTGCATTACCGGTCGATGC-3′ and reverse primer: 5′-CAGGGTGTTATAAGCAATCCCC -3′) transgenic mice. Mice aged 1–3 months were typically used for experiments. Mice were housed at constant temperature with a 12-h/12-h dark/light cycle (lights on at 9 a.m.) and 1–6 mice were kept per cage. All experiments were approved by the institutional animal care and use committee of Chinese Academy of Sciences. Mice of either sex were used and randomly assigned to different groups for all experiments.

**Culture and transfection of primary cells.** Isolation and culture of SPH primary astrocytes were performed at postnatal day 5 as described previously[39]. Mouse embryonic fibroblasts were derived from 13.5 d embryos and maintained in DMEM supplemented with 10% FBS and 1% penicillin/streptomycin (Thermo Fisher Scientific). To determine the activation of *Ascl1, Neurog2* and *Neurod1* (ANN) in SPH primary astrocytes, 1 μg plasmids expressing Cre and mCherry, and 3 μg plasmids expressing sgRNAs targeting ANN factors were co-transfected per well (six-well plate). mCherry-positive cells were collected for qPCR 2–3 d post-transfection. To compare the activation efficiency of SAM, VPR and SPH in primary astrocytes derived from wide type mice, 15 μg plasmids expressing GFP and 15 μg plasmids expressing mCherry, were co-transfected per 10-cm dish. GFP and mCherry double positive cells were collected for qPCR 2 d post-transfection.

**Production of lentivirus and AAV8.** Lentivirus was packaged by transfecting HEK293T cells using Polyethylenimine (PEI) at a final concentration of 50 μg/ml, the ratio of sgRNA-EF1a-Cre-mCherry expressing plasmid (Addgene 52963) and packaging vectors psPAX2 (Addgene 12260) and pMD2.G (Addgene 12259) is 4:3:2. Virus supernatant was collected 2–3 d post-transfection. Astrocytes and fibroblasts were infected using concentrated and fresh supernatant, respectively. A mixture of lentiviral supernatants was used to achieve activation of multiple genes. AAV8 was produced by triple transfection of HEK293T cells using PEI. Viral particles from the media and cells were harvested, purified and concentrated 3–5 d after transfection[22,40]. Maximally 12 sgRNAs could be packaged into one AAV-sgRNAs array due to the packaging limit of AAV, and the titers of AAV-12-sgRNA-array and AAV-10-sgRNA-array were around $5 \times 10^{12}$.

**RNA extraction and qPCR.** Astrocytes and fibroblasts were harvested for Real-Time quantitative PCR 10 d and 2–3 d post-infection, respectively. RNA was extracted using Trizol (Ambion) and subsequently converted to cDNA using a reverse transcription kit HiScript Q RT SuperMix for qPCR (Vazyme, Biotech). qPCR reactions were performed with AceQ qPCR SYBR Green Master Mix (Vazyme, Biotech). RNA extracted from the N2A cells was prepared for RNA-seq experiments, as described previously[7]. The cycle number was set as 40 if the amplification signal could not be detected in control samples (in total of 45 cycles). All primers used for qPCR are listed in Supplementary Table 2.

**Stereotactic injection of AAV8, hydrodynamic tail vein injection and hepatocyte isolation.** *Stereotactic injection of AAV8.* Surgical preparation was performed as previously described[41]. For the purpose of determining the activation in the brain, AAV8 was injected into the cerebral cortex and cerebellar cortex at a depth of 0.3–1.8 mm, and injected brain regions were dissected for qPCR 2 weeks post-injection. For the purpose of direct conversion of astrocytes into neurons, AAV8 was injected into the midbrain at a depth of 0.5–1 mm.

*Hydrodynamic tail vein injection.* 1.5–2.5 ml Ringer's buffer containing approximately 50–200 μg plasmid DNA or 0.5 ml Ringer's buffer containing approximately $3 \times 10^{11}$ transducing units (TU) of AAV was injected into mouse via tail vein[42]. Mice were sacrificed typically 4–6 d post-injection of plasmids or 1–2 weeks post-injection of AAV. Separated liver lobes were homogenized in Trizol using a mechanical tissue homogenizer for RNA extraction, western blot or fixed with 4% of paraformaldehyde for immunofluorescence staining or frozen for western blot.

*Hepatocyte isolation.* Primary hepatocytes were isolated by standard two-step collagenase perfusion method[43] and purified by 40% Percoll (Sigma) at low-speed centrifugation (1,000 rpm, 10 min), mCherry-positive hepatocytes were isolated for qPCR using FACS. Because of the variance of hydrodynamics-based transfection, typically well transfected mice were used for further analysis based on fluorescence expression.

**Immunofluorescence staining and in situ hybridization.** The livers and brains were fixed overnight with 4% paraformaldehyde (PFA), and stored in 30% sucrose for 12 h. After embedding in OCT compound (Sakura Finetek), 10 μm liver sections or 50 μm brain sections were used for immunofluorescence staining. Slices were thoroughly rinsed with 0.1 M PB three times. Primary antibodies used to stain the brain and liver sections were as follows: rabbit monoclonal antibody to HA-tag (Brain, 1:1000, #3724, CST[44]), rabbit polyclonal NeuN antibody (Brain, 1:500, #ABN78, Millipore[45]), mouse monoclonal DsRed2 Antibody (Liver, 1:1,000, #sc-101526, Santa Cruz), mouse monoclonal GS antibody (liver, 1:500, Millipore[46]), rabbit polyclonal antibody to GAPDH (1:2000, #10494-1-AP, Proteintech[47]), rabbit polyclonal CYP2E1antibody (liver, 1:1,000, #ab28146, Genetex[48]), rabbit polyclonal antibody to mCherry (liver, 1:2,000, #GTX128508, Genetex[49]), mouse monoclonal antibody to ASCL1 (liver, 1:2,000, Liver, #556604, BD biosciences[50]), rabbit polyclonal to DKK1 (brain, 1:2,000, #ab61034, Abcam) and rabbit polyclonal antibody to HBB (brain, 1:2,000, #AP11557b, Abgent[51]). The sections were thoroughly rinsed with 0.1 M PB for three times, and subsequently covered with mountant (Life Technology). Double staining combining the in situ hybridization and the fluorescent immunostaining was performed on cryostat sections of the mouse brain, as previously described[52]. *Dkk1* and *Hbb* probes (Supplementary Table 5) were made using T7/SP6 transcriptase (Roche). For in situ hybridization, brain sections were warmed at room temperature and dried at 50 °C for 20 min. Then brain sections were fixed with 4% paraformaldehyde (dissolved in DEPC-PBS) at room temperature for 20 min and washed twice with DEPC-PBS for 5 min. And treated with 2 μg/ml and 1 μg/ml proteinase K (dissolved in PK buffer) for 5 min, respectively. Prehybridization was performed at 67 °C and replaced with 1 μg/ml of probe in hybridization buffer. After 12–16 h incubation, brain sections were washed with SSC at 67 °C and free probes were digested with 3 μg/ml RNase at 37 °C for 30 min. Brain slices were blocked in 10% heat inactivated sheep serum and incubated in anti-digoxygenin antibody (1:2,000, #11093274910, Roche, diluted in 10% sheep serum[53]). For immunostaining, antigens were retrieved in 0.01 M sodium citrate at 80 °C for 20 min and blocked in TBS containing 0.4% Triton X-100 and 10% goat serum. Primary antibody (rabbit-DsRed, #632496, 1:500, Takara) and secondary antibody (donkey anti rabbit, 1:200, Jackson Immunoresearch #711-166-152[54]) were used to amplify the mCherry signal.

**Electrophysiology.** The detailed recording method was previously described[55]. Briefly, SPH;GFAP-Cre mice (ages 2–3 months, 1–2 months post-infection of

AAV8) were anesthetized by intraperitoneal injection of pentobarbital sodium (40 mg/kg) and then transcardial perfused with 25–30 ml of room temperature carbogenated NMDG artificial cerebrospinal fluid (aCSF) [NMDG aCSF (mM): NMDG 92, KCl 2.5, $NaH_2PO_4$ 1.25, $NaHCO_3$ 30, HEPES 20, glucose 25, thiourea 2, sodium ascorbate 5, sodium pyruvate 3, $CaCl_2$ 0.5, $MgSO_4$ 10]. The brains were gently extracted from the skull after perfusion within 1 min and placed into the icy-cold NMDG aCSF solution for an additional 30 s. The brain tissues were then trimmed and sectioned with Leica VT1200S at 250–350 μm thickness in the slicing chamber filled with icy-cold NMDG aCSF solution bubbled with 95%$O_2$/5%$CO_2$. The advance speed was set at 0.04–0.05 mm/s with the amplitude of 1 mm. The total time for the slicing procedure should be less than 15 min. Slices were transferred into a holding chamber containing carbogenated NMDG aCSF and kept there for ≤12 min at 32–34 °C for the initial protective recovery. After the initial recovery period, the slices were transferred into a new holding chamber containing room-temperature HEPES holding aCSF [HEPES holding aCSF (mM): NaCl 92, KCl 2.5, $NaH_2PO_4$ 1.25, $NaHCO_3$ 30, HEPES 20, glucose 25, thiourea 2, sodium ascorbate 5, sodium pyruvate 3, $CaCl_2$ 2, $MgSO_4$ 2] under constant carbogenation. After about 1 h, the slices can be transferred into the recording chamber filled with recording solution [recording aCSF (mM): NaCl 119, KCl 2.5, $NaH_2PO4$ 1.25, $NaHCO_3$ 24, glucose 12.5, $CaCl_2$ 2, $MgSO_4$ 2] under the microscope Olympus BX51WI. The recording was acquired through Clampex 10 equipped with Axon 700B and Digidata1550A. The internal solution is composed of (mM) potassium gluconate 126, KCl 2, $MgCl_2$ 2, HEPES 10, EGTA 0.2, $Na_2$-ATP 4, $Na_3$-GTP 0.4, creatine phosphate 10. The temperature was maintained at 32 °C during the recording. Recordings were made in the inferior colliculus central nucleus (ICC) of the dorsal midbrain. The morphology and mCherry expression were visualized by an upright microscope, to select mature iNs for patch-clamp recordings.

**RNA-seq data analysis.** High-throughput mRNA sequencing (RNA-seq) was carried out using Illumina Genome Analyzer. Trimmomatic (v0.36) was used to remove adapters during sequencing. Qualified reads were mapped to the mouse reference genome (mm10) by hisat2 (v2.0.0) with default parameters. Next, stringtie (v2.0) was conducted to estimate the gene expression levels on the alignment file and gene abundances were reported in FPKM (fragments per kilobase of transcript per million fragments mapped). All data are available with the SRA accession number SRP118855.

**Single-cell RNA-seq.** Primary astrocytes derived from the SPH mice were transfected with1ug all-in-one plasmid per well (24-well plate). Single mCherry-positive astrocytes were selected by glass pipettes, 60 h post-transfection. RNA isolation and library construction were performed as described previously[56]. Cells with high-quality libraries were used for further analysis. For the single-cell amplification sequencing data, smart adapters produced during DNA amplification were also removed in addition to Illumina adapters before subsequent analysis. All data are available with the SRA accession number SRP118855.

**Inverse PCR.** Genomic DNA from mouse tail was isolated and digested with MspI enzyme for 3 h. Then the digested DNA was ligated for 3 h, followed by one round of nest PCR. The PCR products were run on a 1.5% agarose gel, clear bands were excised, purified and ligated to Pmd-19T-vectors. Single clones were picked for sequencing.

**Statistical analysis.** All values are shown as mean ± s.e.m. One-way ANOVA followed by Tukey's test and unpaired two-tailed Student's *t* test were used for comparisons and $P < 0.05$ was considered to be statistically significant. Randomization was used in all experiments and no statistical methods were used to pre-determine sample sizes but our sample sizes are similar to those reported in previous publications[19]. Data distribution was assumed to be normal but this was not formally tested. Data collection and analysis were not performed blind to the conditions of the experiments.

**Life Sciences Reporting Summary.** Information on experimental details can be found in the Life Sciences Reporting Summary.

**Accession codes.** RNA-seq and single-cell RNA-seq data are available with the SRA accession number SRP118855.

**Data availability.** The SPH transgenic mice will be donated to the Jackson Laboratory (https://www.jax.org/) and Shanghai Model Organism Center (http://www.shmo.com.cn/). RNA-seq and single-cell RNA-seq data are available with the SRA accession number SRP118855. Other data that support the findings of this study are available from the corresponding author upon reasonable request.

## References


38. Ding, S. et al. Efficient transposition of the *piggyBac* (PB) transposon in mammalian cells and mice. *Cell* **122**, 473–483, https://doi.org/10.1016/j.cell.2005.07.013 (2005).
39. McCarthy, K. D. & de Vellis, J. Preparation of separate astroglial and oligodendroglial cell cultures from rat cerebral tissue. *J. Cell. Biol.* **85**, 890–902, https://doi.org/10.1083/Jcb.85.3.890 (1980).
40. Deverman, B. E. et al. Cre-dependent selection yields AAV variants for widespread gene transfer to the adult brain. *Nat. Biotechnol.* **34**, 204–209, https://doi.org/10.1038/nbt.3440 (2016).
41. Zhou, H. et al. Cerebellar modules operate at different frequencies. *Elife* **3**, e02536, https://doi.org/10.7554/eLife.02536 (2014).
42. Liu, F., Song, Y. & Liu, D. Hydrodynamics-based transfection in animals by systemic administration of plasmid DNA.*Gene Ther.* **6**, 1258–1266, https://doi.org/10.1038/sj.gt.3300947 (1999).
43. Huang, P. et al. Induction of functional hepatocyte-like cells from mouse fibroblasts by defined factors. *Nature* **475**, 386–389, https://doi.org/10.1038/nature10116 (2011).
44. Yang, S. et al. MANF regulates hypothalamic control of food intake and body weight. *Nat. Commun.* **8**, 579, https://doi.org/10.1038/s41467-017-00750-x (2017).
45. Lundgaard, I. et al. Direct neuronal glucose uptake heralds activity-dependent increases in cerebral metabolism. *Nat. Commun.* **6**, 6807, https://doi.org/10.1038/ncomms7807 (2015).
46. Greferath, U. et al. Inner retinal change in a novel rd1-FTL mouse model of retinal degeneration. *Front. Cell. Neurosci.* **9**, 293, https://doi.org/10.3389/fncel.2015.00293 (2015).
47. Wang, P. et al. Dual role of Ski in pancreatic cancer cells: tumor-promoting versus metastasis-suppressive function. *Carcinogenesis* **30**, 1497–1506, https://doi.org/10.1093/carcin/bgp154 (2009).
48. McCracken, J. M. et al. C57BL/6 substrains exhibit different responses to acute carbon tetrachloride exposure: implications for work involving transgenic mice. *Gene Expr.* **17**, 187–205, https://doi.org/10.3727/105221617X695050 (2017).
49. Yao, X. et al. Homology-mediated end joining-based targeted integration using CRISPR/Cas9. *Cell. Res.* **27**, 801–814, https://doi.org/10.1038/cr.2017.76 (2017).
50. Ivaniutsin, U., Chen, Y., Mason, J. O., Price, D. J. & Pratt, T. Adenomatous polyposis coli is required for early events in the normal growth and differentiation of the developing cerebral cortex. *Neural Dev.* **4**, 3, https://doi.org/10.1186/1749-8104-4-3 (2009).
51. Ou, Z. et al. The combination of CRISPR/Cas9 and iPSC technologies in the gene therapy of human β-thalassemia in mice. *Sci. Rep.* **6**, 32463, https://doi.org/10.1038/srep32463 (2016).
52. Huang, M. et al. Ptf1a, Lbx1 and Pax2 coordinate glycinergic and peptidergic transmitter phenotypes in dorsal spinal inhibitory neurons. *Dev. Biol.* **322**, 394–405, https://doi.org/10.1016/j.ydbio.2008.06.031 (2008).
53. Schinko, J., Posnien, N., Kittelmann, S., Koniszewski, N. & Bucher, G. Single and double whole-mount in situ hybridization in red flour beetle (*Tribolium*) embryos. *Cold Spring Harb. Protoc.* **2009**, t5258, https://doi.org/10.1101/pdb.prot5258 (2009).
54. Ramer, M. S. Anatomical and functional characterization of neuropil in the gracile fasciculus. *J. Comp. Neurol.* **510**, 283–296, https://doi.org/10.1002/cne.21785 (2008).
55. Ting, J. T., Daigle, T. L., Chen, Q. & Feng, G. Acute brain slice methods for adult and aging animals: application of targeted patch clamp analysis and optogenetics. *Methods Mol. Biol.* **1183**, 221–242, https://doi.org/10.1007/978-1-4939-1096-0_14 (2014).
56. Li, C. L. et al. Somatosensory neuron types identified by high-coverage single-cell RNA-sequencing and functional heterogeneity. *Cell. Res.* **26**, 83–102, https://doi.org/10.1038/cr.2015.149 (2016).

nature research

Corresponding author(s): Hui Yang, Pengyu Huang

☐ Initial submission ☐ Revised version ☒ Final submission

# Life Sciences Reporting Summary

Nature Research wishes to improve the reproducibility of the work that we publish. This form is intended for publication with all accepted life science papers and provides structure for consistency and transparency in reporting. Every life science submission will use this form; some list items might not apply to an individual manuscript, but all fields must be completed for clarity.

For further information on the points included in this form, see Reporting Life Sciences Research. For further information on Nature Research policies, including our data availability policy, see Authors & Referees and the Editorial Policy Checklist.

## Experimental design

1. Sample size

Describe how sample size was determined.

Unpaired T-test (two-tailed) and one-way Anova followed by Tuky's test were used to determine the significance. Sample sizes in this manuscript were similar to previous papers (Chavez, A. et al., Nature Methods, 2016. Konermann S. et al., Nature, 2015).

2. Data exclusions

Describe any data exclusions.

In methods. Poor transfected/infected mice were excluded.

3. Replication

Describe whether the experimental findings were reliably reproduced.

All attempts at replication were successful.

4. Randomization

Describe how samples/organisms/participants were allocated into experimental groups.

Randomization was used in all experiments.

5. Blinding

Describe whether the investigators were blinded to group allocation during data collection and/or analysis.

To compare the fluorescence intensity of different activators, BFP-positive cells were selected and analyzed randomly per group(Figure 1), blindness was not used in other experiments. However, all samples were collected and all data were analyzed in an unbiased manner.

Note: all studies involving animals and/or human research participants must disclose whether blinding and randomization were used.

6. Statistical parameters

For all figures and tables that use statistical methods, confirm that the following items are present in relevant figure legends (or in the Methods section if additional space is needed).

| n/a | Confirmed |
|---|---|
| ☐ | ☒ The exact sample size (*n*) for each experimental group/condition, given as a discrete number and unit of measurement (animals, litters, cultures, etc.) |
| ☐ | ☒ A description of how samples were collected, noting whether measurements were taken from distinct samples or whether the same sample was measured repeatedly |
| ☐ | ☒ A statement indicating how many times each experiment was replicated |
| ☐ | ☒ The statistical test(s) used and whether they are one- or two-sided (note: only common tests should be described solely by name; more complex techniques should be described in the Methods section) |
| ☐ | ☒ A description of any assumptions or corrections, such as an adjustment for multiple comparisons |
| ☐ | ☒ The test results (e.g. *P* values) given as exact values whenever possible and with confidence intervals noted |
| ☐ | ☒ A clear description of statistics including central tendency (e.g. median, mean) and variation (e.g. standard deviation, interquartile range) |
| ☐ | ☒ Clearly defined error bars |

*See the web collection on statistics for biologists for further resources and guidance.*

## Software

Policy information about availability of computer code

7. Software

| | |
|---|---|
| Describe the software used to analyze the data in this study. | Custom algorithms or software was not used in this study.<br>Fluorescence intensity: Zen (zeiss)<br>Flow cytometry: FlowJo<br>RNA-seq: Illumina Genome Analyzer, Trimmomatic (v0.36), Hisat2 (v2.0.0), Stringtie (v2.0)<br>Western Blot: Image J<br>Electrophysiology: Clampex 10<br>Statistics: SPSS 17.0 |

For manuscripts utilizing custom algorithms or software that are central to the paper but not yet described in the published literature, software must be made available to editors and reviewers upon request. We strongly encourage code deposition in a community repository (e.g. GitHub). *Nature Methods* guidance for providing algorithms and software for publication provides further information on this topic.

## Materials and reagents

Policy information about availability of materials

8. Materials availability

| | |
|---|---|
| Indicate whether there are restrictions on availability of unique materials or if these materials are only available for distribution by a for-profit company. | The SPH transgenic mice will be donated to the jackson laboratory (https://www.jax.org/) and Shanghai Model Organism Center Inc., Shanghai, China (http://www.shmo.com.cn/). Other materials are available upon reasonable request. |

9. Antibodies

| | |
|---|---|
| Describe the antibodies used and how they were validated for use in the system under study (i.e. assay and species). | rabbit monoclonal antibody to HA-tag (Brain, 1:1000, #3724, CST, ref. 45), rabbit polyclonal NeuN antibody (Brain, 1:500, #ABN78, Millipore, ref. 46), mouse monoclonal DsRed2 Antibody (Liver, 1:1000, #sc-101526, Santa cruz), mouse monoclonal GS antibody (liver, 1:500, Millipore, ref. 47), rabbit polyclonal antibody to GAPDH (1:2000, #10494-1-AP, Proteintech, ref. 48), rabbit polyclonal CYP2E1antibody (liver, 1:1000, #ab28146, Genetex, ref. 49), rabbit polyclonal antibody to mCherry (liver, 1:2000, #GTX128508, Genetex, ref. 50), mouse monoclonal antibody to ASCL1 (liver, 1:2000, Liver, #556604, BD biosciences, ref. 51), rabbit polyclonal to DKK1 (brain, 1:2000, #ab61034, Abcam) and rabbit polyclonal antibody to HBB (brain, 1:2000, # AP11557b, Abgent, ref. 52, anti-digoxygenin antibody (1:2000, #11093274910, Roche, ref. 54). |

10. Eukaryotic cell lines

| | |
|---|---|
| a. State the source of each eukaryotic cell line used. | Cell bank, Shanghai Institute of Biochemistry and Cell Biology, Chinese Academy of Sciences |
| b. Describe the method of cell line authentication used. | Cell lines were authenticated by the supplier. |
| c. Report whether the cell lines were tested for mycoplasma contamination. | Cell lines were tested for mycoplasma contamination. |
| d. If any of the cell lines used are listed in the database of commonly misidentified cell lines maintained by ICLAC, provide a scientific rationale for their use. | None of the cell lines used was listed in the database of ICLAC. |

## Animals and human research participants

Policy information about studies involving animals; when reporting animal research, follow the ARRIVE guidelines

### 11. Description of research animals

Provide details on animals and/or animal-derived materials used in the study.

Cre-dependent SPH transgenic mice were generated with piggyBac transposon system in F1 zygotes. Three chimeric male founders were selected to cross with wild type C57BL/6 mice. SPH;GFAP-Cre double-transgenic mice were generated by crossing SPH transgenic mice with GFAP-Cre (JAX stock #004600, forward primer: 5'-GCCTGCATTACCGGTCGATGC-3' and reverse primer: 5'-CAGGGTGTTATAAGCAATCCCC -3') transgenic mice. Mice aged 1-3 months were typically used for experiments. Mice were housed at constant temperature with a 12 h/12 h dark/light cycle (lights on at 9 a.m.) and 1-6 mice were kept per cage. All experiements were approved by the institutional animal care and use committee of Chinese Academy of Sciences. Mice of either sex were used and randomly assigend to different groups for all experiments.

Policy information about studies involving human research participants

### 12. Description of human research participants

Describe the covariate-relevant population characteristics of the human research participants.

No human participants.

nature research

Corresponding author(s): Hui Yang, Pengyu Huang

☐ Initial submission ☐ Revised version ☒ Final submission

# Flow Cytometry Reporting Summary

Form fields will expand as needed. Please do not leave fields blank.

## Data presentation

For all flow cytometry data, confirm that:

☒ 1. The axis labels state the marker and fluorochrome used (e.g. CD4-FITC).

☒ 2. The axis scales are clearly visible. Include numbers along axes only for bottom left plot of group (a 'group' is an analysis of identical markers).

☒ 3. All plots are contour plots with outliers or pseudocolor plots.

☒ 4. A numerical value for number of cells or percentage (with statistics) is provided.

## Methodological details

| | |
|---|---|
| 5. Describe the sample preparation. | Cell were digested by trypsin (0.05%), contrifuged at 1000 rpm and filtered with a 35μm nylon mesh. (Supplementary Figure 2b) |
| 6. Identify the instrument used for data collection. | MoFlo XDP (Beckman) |
| 7. Describe the software used to collect and analyze the flow cytometry data. | Collect: Summit Software version 5.2<br>Analyze: FlowJo |
| 8. Describe the abundance of the relevant cell populations within post-sort fractions. | 20000 cells were sorted per group. Positive and negative boundaries were determined by control cells that were not transfected with any plasmids. |
| 9. Describe the gating strategy used. | Positive and negative boundaries were determined by control cells that were not transfected with any plasmids. |

Tick this box to confirm that a figure exemplifying the gating strategy is provided in the Supplementary Information. ☒